

## Voltage Regulation of Boost Converter using Observer based Sliding Mode Controller

Ramadhani Kurniawan Subroto\*<sup>1</sup>, Sapriesty Nainy Sari<sup>2</sup>, Zainul Abidin<sup>3</sup>, Kuo Lung Lian<sup>4</sup>

<sup>1,2,3</sup>Department of Electrical Engineering, Brawijaya University, MT Haryono St. 167 Malang, Indonesia

<sup>4</sup>Department of Electrical Engineering, National Taiwan University of Science and Technology,  
No. 43, Section 4, Keelung Rd, Da'an District, Taipei City, Taiwan 10607

\*Corresponding author, e-mail: ramasubroto@ub.ac.id

### Abstract

*This study dealt with output voltage regulation of boost converter using observer based sliding mode controller comprises of adaptive PI sliding surface. Observer was designed to estimate the inductor current value, such that no sensor was required as a feedback. Adaptive PI sliding surface was constructed from the difference between estimated inductor current and its reference value. The stability of proposed method was ensured by using Lyapunov direct method. To test the system performance, numerical simulation was conducted. The result indicated that the integral absolute error value of proposed method was 0.19, which was 7 times less than sliding mode with PI sliding surface. Consequently, the proposed method was able to estimate accurately the inductor value, track the reference voltage perfectly, and show its robustness against parameter variations.*

**Keywords:** boost converter, observer, sliding mode control, voltage regulation

**Copyright © 2018 Universitas Ahmad Dahlan. All rights reserved.**

### 1. Introduction

Research focus on power electronics has been growing rapidly due to the more extensively developed renewable energy sources [1]. This is the reason why power electronics devices, such as dc-dc converters, have to be better day by day in order to have maximum efficiency and well-controlled. In general, dc-dc converters are employed to alter the voltage level from renewable energy sources to voltage level consumed by either load or grid [2, 3]. There are many types of dc-dc converter, namely buck [4], boost [5], buck-boost [6], SEPIC [7], Cuk [8], and Zeta [9] converters. Among the others, boost converter is the most widely applied converter, which is able to raise the voltage level. Since boost converter comprises an active component (MOSFET/IGBT) and some passive components (resistor, inductor, and capacitor), regulating the output voltage this converter is quite challenging. In addition, this converter also has nonlinear and non-minimum phase features, in which the controlling of output voltage is not able to be done directly such that inductor current is entailed to regulate it [5]. Consequently, the inductor current needs to be measured continuously by using sensors. The problem arises when the additional sensor is installed to measure inductor current. It is very vulnerable to noise and can lead to precision error. Besides, it also can increase the production cost and space requirement. Therefore, the observer is proposed to estimate the inductor current continuously such that no sensor is required for real time measurement.

Several control strategies have been conducted for voltage regulation of boost converters, e.g., PID control [10-13], adaptive control [14, 15], robust control [16, 17]. There are some drawbacks in using those methods. The procedures for obtaining the control parameters require linearization is some certain operating points, which results narrowness of the operating points. Consequently, the converter is not able to reach all operating range and conditions. To deal with nonlinear system, like boost converter, intelligent control [18-22] strategies have been applied to cope with this problem. However, the stability of this controller is not able to be analyzed. Other approaches are by using Sliding Mode Control [5, 23-29] strategy to control the output voltage of boost converter. Unlike other controllers, this controller offers good robustness and stability for nonlinear system, especially boost converter [5, 23-29]. In the previous works, the sliding surface is static, whose parameters are fixed. In order to enhance the system

performance to be more responsive, fast, and robust; this study applies the dynamic sliding surface, whose parameters are able to change as the system parameters change. The research on dynamic sliding surface has been successfully applied in [30], but there are no literatures discussing and implementing the combination of this method with observer on boost converter. Therefore, the main contribution of this paper is emphasized on how to design the sliding mode controller which has adaptive sliding surface to regulate the output voltage without sensor necessity.

## 2. Proposed Method

The mathematical model of boost converter and the procedures in how to design the proposed observer and controller are described in this section.

### 2.1. Observer Design

Boost converter's equivalent circuit is depicted in Figure 1. Both Kirchoff current and voltage laws are employed to obtain the mathematical model of this converter, which results nonlinear features [5]. The deeper explanation in how to obtain the dynamic model of this converter is studied in [2, 5]. This converter is assumed to be an ideal model, in which parasitic effects are not taken into account. In addition, this converter is also regarded in continuous conduction mode (CCM), in which the inductor current never reaches zero or always be positive. As a consequence of those assumptions, the mathematical model of this converter can be obtained as

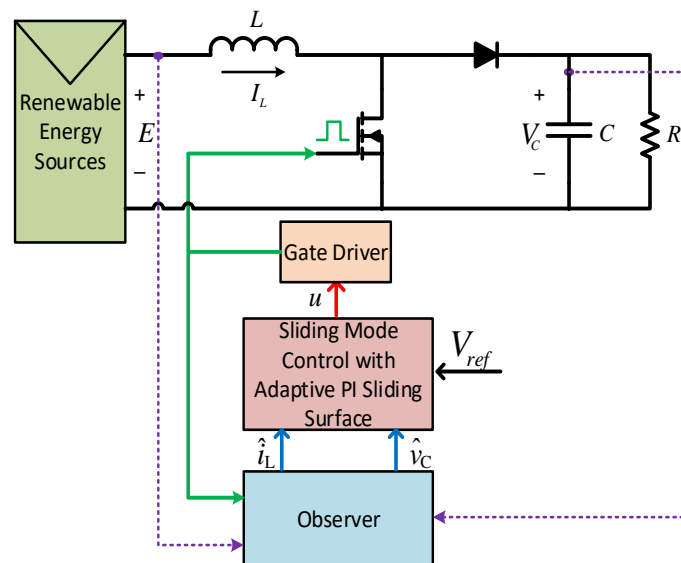


Figure 1. Block diagram of proposed method

$$\begin{aligned} \dot{v}_C &= -\frac{v_C}{RC} + \frac{i_L}{C}(1-d) \\ \dot{i}_L &= \frac{E}{L} - \frac{v_C}{L}(1-d) \end{aligned} \quad (1)$$

where  $i_L$  and  $v_C$  express inductor current and output voltage, respectively;  $E$  represents input voltage;  $d$  denotes control input, in the form of duty ratio; and  $R, L, C$  indicate resistor, inductor, and capacitor, respectively.

In this study, the observer of the converter is employed to estimate the proper value of the inductor current and output voltage. Thus, the characteristics of observer has to resemble the real plant. Therefore, the observer is constructed as

$$\begin{aligned}\dot{\hat{v}}_C &= -\frac{\hat{v}_C}{RC} + \frac{\dot{\hat{i}}_L}{C}(1-d) + \Gamma(v_C - \hat{v}_C) \\ \dot{\hat{i}}_L &= \frac{E}{L} - \frac{\hat{v}_C}{L}(1-d)\end{aligned}\quad (2)$$

where  $\Gamma$  represent an observer gain;  $\hat{v}_C$  and  $\hat{i}_L$  denote the estimates of  $v_C$  and  $i_L$ , respectively. By defining estimation errors as  $\tilde{v}_C = v_C - \hat{v}_C$  and  $\tilde{i}_L = i_L - \hat{i}_L$ . Thus, the estimator error dynamics can be obtained as

$$\begin{aligned}\dot{\tilde{v}}_C &= -\frac{\tilde{v}_C}{RC} + \frac{\tilde{i}_L}{C}(1-d) - \Gamma\tilde{v}_C \\ \dot{\tilde{i}}_L &= -(1-d)\frac{\tilde{v}_C}{L}\end{aligned}\quad (3)$$

## 2.2. Sliding Mode Control with Adaptive PI Sliding Surface

The most important part in designing the sliding mode control is the sliding (switching) surface structure. Sliding surface is determined to force the states from any initial points to the equilibrium. Therefore, this is a crucial factor for control engineers requiring to be considered. A fundamental method in designing observer and controller is focused on Lyapunov stability. The procedure to obtain proposed controller is as follows:

Step 1: Determine the observer gain value in sense of Lyapunov stability

A positive definite of Lyapunov function is selected as

$$V = \frac{1}{2}C\tilde{v}_C^2 + \frac{1}{2}L\tilde{i}_L^2 \quad (4)$$

afterwards, the time derivative of (4) is obtained

$$\dot{V} = C\tilde{v}_C\dot{\tilde{v}}_C + L\tilde{i}_L\dot{\tilde{i}}_L \quad (5)$$

by incorporating (3) into (5), it results

$$\dot{V} = -\left(\frac{1}{R} + \Gamma C\right)\tilde{v}_C^2 \quad (6)$$

in order to achieve stable in sense of Lyapunov, equation in the bracket should be positive definite. Consequently, it can be determined that

$$\Gamma > -\frac{1}{RC} \quad (7)$$

Step 2: Determine the sliding surface

In this paper, the PI structure is adapted to construct the sliding surface. There are two types of PI sliding surface compared, namely static and dynamic sliding surface. The words "static" and "dynamics" refers to the characteristics of the controller parameters. In static sliding surface, the parameters are determined as constants, while in dynamic, the parameters can be varying regarding to the adaptive mechanism and parameter variations occurrence. Therefore, the sliding surface for adaptive PI is designed as

$$\zeta(t) = \hat{i}_L(t) - I_{Lref} + \hat{\psi}(t) \int_0^t \hat{i}_L(\tau) - I_{Lref} d\tau \quad (8)$$

where  $I_{Lref}$  represents inductor current reference and  $\hat{\psi}$  denotes sliding surface parameter, which varies in time. Inductor current reference is defined as

$$I_{Lref} = \frac{V_{ref}^2}{RE} \quad (9)$$

meanwhile, the sliding surface for static PI is simply constructed as

$$\zeta(t) = \hat{i}_L(t) - I_{Lref} + \psi \int_0^t (\hat{i}_L(\tau) - I_{Lref}) d\tau \quad (10)$$

where  $\psi$  represents the constant sliding surface parameter. Thus, the difference between (8) and (10) is only in sliding surface parameter  $\psi$ .

Step 3: Obtaining the control signal

In sliding mode control, there are types of control signal, namely equivalent and natural control signal. The equivalent control signal is resulted from the time derivative of sliding surface. By defining control error as  $e = \hat{i}_L - I_{Lref}$  and substituting it into (10), it allows

$$\dot{\zeta} = \dot{e} + \psi e = 0 \quad (11)$$

consequently, the equivalent control signal for PI sliding surface can be obtained as

$$d_{eq} = 1 - \frac{L}{\hat{v}_C} \left( \frac{E}{L} + \psi e \right) \quad (12)$$

the natural control signal can be derived from Lyapunov function as

$$V = \frac{1}{2} \zeta^2 \quad (13)$$

by taking time derivative of (12), it can be obtained

$$d_n = -\frac{L}{\hat{v}_C} \text{sgn}(\zeta) \quad (14)$$

where  $\text{sgn}(\ )$  denotes signum function. Therefore, the control signal for PI sliding surface becomes

$$d = d_{eq} + d_n = 1 - \frac{L}{\hat{v}_C} \left( \frac{E}{L} + \psi e + \text{sgn}(\zeta) \right) \quad (15)$$

on the other hand, by modifying (15) into (16) and assuming that (16) is the control signal for adaptive PI sliding surface as

$$d = 1 - \frac{L}{\hat{v}_C} \left( \frac{E}{L} + \hat{\psi} e + \hat{\lambda} \text{sgn}(\zeta) \right) \quad (16)$$

where  $\hat{\lambda}$  is the switching gain parameters, which varies in time. It can be clearly seen that another problem arises in determining the  $\hat{\psi}$  and  $\hat{\lambda}$

Step 4: Obtaining the adaptive mechanism for  $\hat{\psi}$  and  $\hat{\lambda}$

The adaptive mechanism for these parameters is obtained by using Lyapunov method. Time derivative of (8) can be obtained

$$\dot{\zeta} = \dot{e} + \hat{\psi}e + \hat{\psi} \int_0^t e(\tau) d\tau \quad (17)$$

by incorporating (16) into (17), it results

$$\dot{\zeta} = -\hat{\lambda} \operatorname{sgn}(\zeta) + \hat{\psi} \int_0^t e(\tau) d\tau \quad (18)$$

the Lyapunov function is introduced as

$$V = \frac{1}{2} \zeta^2 + \frac{1}{2} \beta \tilde{\lambda}^2 \quad (19)$$

where  $\beta$  can be assumed as positive definite constant and  $\tilde{\lambda}$  is estimation error of  $\lambda$ , which is defined as

$$\tilde{\lambda} = \hat{\lambda} - \lambda \quad (20)$$

time derivative of (19) is achieved as

$$\dot{V} = \zeta \dot{\zeta} + \beta \tilde{\lambda} \dot{\tilde{\lambda}} \quad (21)$$

by substituting (18) and (20) into (21), it is obtained

$$\dot{V} = -\hat{\lambda} |\zeta| + \hat{\psi} \zeta \int_0^t e(\tau) d\tau + \beta \hat{\lambda} \dot{\tilde{\lambda}} - \beta \lambda \dot{\tilde{\lambda}} \quad (22)$$

Since (20) has to be negative definite to satisfy Lyapunov stability,  $\dot{\hat{\psi}}$  and  $\dot{\hat{\lambda}}$  are obtained

$$\dot{\hat{\psi}} = -\gamma \zeta \int_0^t e(\tau) d\tau \quad (23)$$

$$\dot{\hat{\lambda}} = \frac{1}{\beta} |\zeta| \quad (24)$$

where  $\gamma$  is any positive definite constant. As a result, the time derivative of Lyapunov (22) becomes

$$\dot{V} = -\gamma \zeta^2 \left( \int_0^t e(\tau) d\tau \right)^2 - \lambda |\zeta| \quad (25)$$

thus, it is theoretically concluded that adaptive sliding surface for sliding mode controller aimed for boost converter is asymptotically stable.

### 3. Research Method

Figure 1 depicts the block diagram of whole system. It can be clearly seen that the system does not require inductor current sensor. The input voltage and output voltage are fed to the observer obtained as (2) to estimate the inductor current value. Consequently, the sensor can be replaced and inductor current value can be accurately obtained. The inductor current and output voltage estimation values are considered for controller design. The proposed controller provides gating signal obtained as (16) that is able to drive the MOSFET such that the output voltage can follow the desired reference voltage eventhough there are many disturbances occur in this system.

The selection of parameters is considered based on (7), (19), and (23), which are derived from Lyapunov stability. Table 1 provides the system parameter used in this research. In Table 1, the parameters include boost converter, sliding mode control with adaptive PI sliding surface, and sliding mode control with PI sliding surface. To verify the proposed method, the numerical simulation is conducted to provide clear and detail descriptions about its properties. In this paper, there are two types of sliding surfaces designed for sliding mode control. As a result, there are further detail discussions about the advantages and drawbacks of those surfaces which are later to be described in Section 4.

Table 1. System Parameters

System	Parameter	Symbol	Value	Units
Boost converter	Inductor	$L$	1.5	mH
	Capacitor	$C$	20	$\mu\text{F}$
	Resistor load	$R$	25	$\Omega$
	Input DC voltage	$E$	12	V
Adaptive PI Sliding Surface	Observer gain	$\Gamma$	1000	-
	Adaptive gains	$\gamma$	0.01	-
		$\beta$	$6 \times 10^{-6}$	-
PI Sliding Surface	Observer gain	$\Gamma$	1000	-
	Controller gain	$\psi$	100	-

#### 4. Results and Analysis

The performance of both systems are proved through simulation, such that comprehensive results are acquired. There are two types of system testing used in this paper. Firstly, the system is tested by varying input voltage, resistor load, and reference voltage simultaneously in the same time frame. The simulation time is set to be 0.9 seconds. Figure 2 illustrates the reference voltage, resistor load, and reference voltage changes applied for system testing. The reference voltage is increased by 20V to 70V at  $t = 0.45$  s. In addition, there are many fluctuations on input voltage and resistor load. In the first 0.15 seconds, the input voltage is kept to be constant to 12V, then it is raised to 27V before its dropping by 25% at  $t = 0.6$  s. At the same time, the resistor load doubled from its nominal value in the first 0.3 seconds before its fall to  $62.5\Omega$  at  $t = 0.75$  s. Secondly, by using simulation time 0.3 seconds, the resistor load and input voltage are varied at  $t = 0.15$  s.

Figure 3 depicts the comparison of output voltage boost converter between adaptive PI sliding surface and PI sliding surface. Clearly, the performance of sliding mode control with adaptive PI sliding surface is better than PI sliding surface in terms of voltage deviation and time. Although there are any load and input voltage variations, the output voltage of boost converter with adaptive PI sliding surface is able to return to the desired voltage value in less than 6 ms. This can be considered extremely fast compared to PI sliding surface, in which the difference is quite significant almost 19 times faster when the input voltage rises to 2.25 times from its nominal value. The same thing also goes to voltage deviation. Voltage deviation ( $\Delta V$ ) is defined as the difference between peak value and reference value. The largest gap of voltage deviation occurs when the resistor load value is added by  $25\Omega$  to  $75\Omega$ , in which the difference is almost double. The summary of this testing is clearly provided in Table 2. To measure the performance quality, Integral Absolute Error (IAE) is employed. It is clearly seen that the IAE value of adaptive PI sliding surface is about 7 times less than PI sliding surface. Thus, this also indicates that proposed method generates fast, robust, and smooth response for boost converter voltage regulation.

Table 2. Performance Specification of Overall Conditions

	IAE	Starting		Adding $E$		Adding $R$		Change $V_{ref}$		Reducing $E$		Reducing $R$	
		$\Delta V$ (V)	$t_s$ (ms)	$\Delta V$ (V)	$t_{rec}$ (ms)	$\Delta V$ (V)	$t_{rec}$ (ms)	$\Delta V$ (V)	$t_s$ (ms)	$\Delta V$ (V)	$t_{rec}$ (ms)	$\Delta V$ (V)	$t_{rec}$ (ms)
Adaptive PI Sliding Surface	0.19	0	5.89	22.70	2.5	15.88	4	0	3.3	1.23	1.5	2.18	2.1
PI Sliding Surface	1.32	0	47.95	23.91	47.3	31.28	55.1	0	39.5	3.25	24.6	5.09	28.6

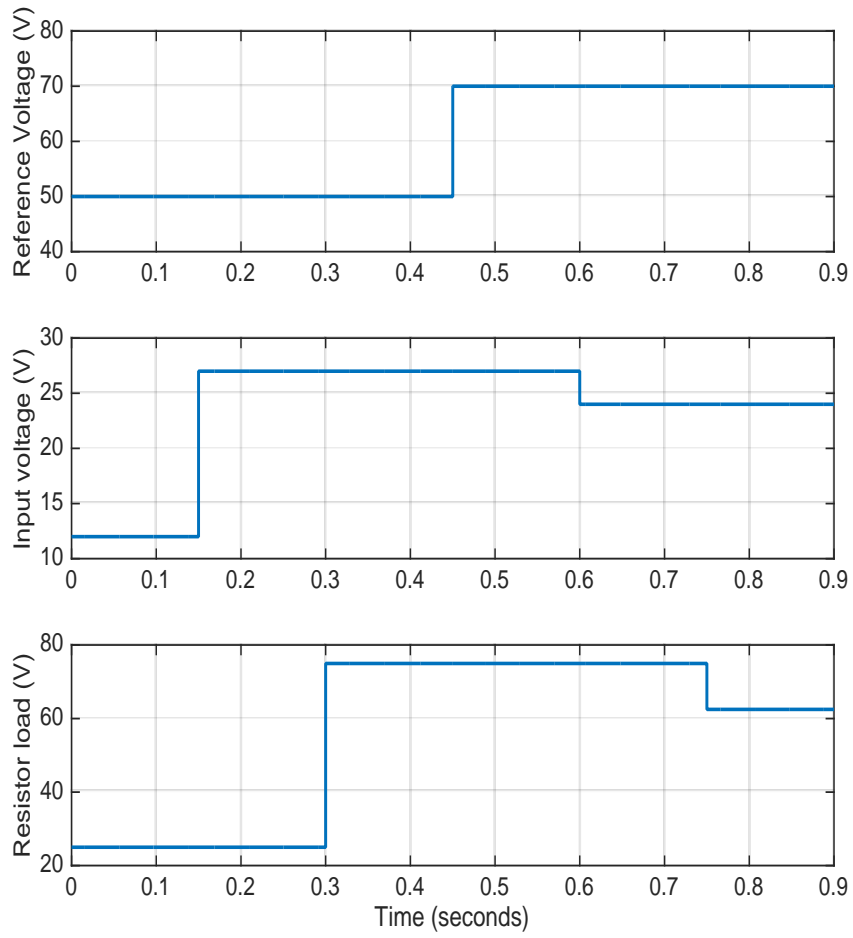


Figure 2. Reference voltage, input voltage, and resistor load variations

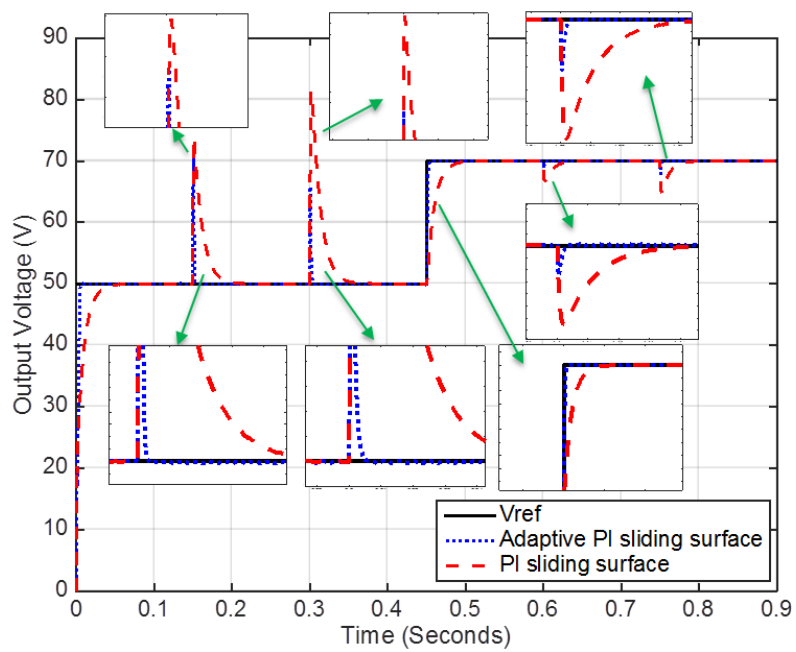


Figure 3. Output voltage response

The comparison results of load variation and input voltage variation testing are presented in Table 3 and Table 4, respectively. Overall, IAE ratio of both methods experiences gradual increase when the load and input voltage are rised. However, eventhough the adaptive PI sliding surface has shorter recovery time and smaller IAE compared to PI sliding surface, its voltage deviation is quite large for the load added not less than its double. When the load is added more than its double, adaptive PI sliding surface shows its effectiveness. The same thing also happened to input voltage variations, in which the small changes in input voltage lead the voltage deviates quite large. On the other hand, when there is a significant increment of input voltage more than its double, the performance of adaptive PI sliding surface produces the best result regarding to voltage deviation, recovery time, and IAE.

Table 3. Performance Specification Regarding to Load Variations

Load added in %	Adaptive PI Sliding Surface			PI Sliding Surface		
	$\Delta V$ (V)	$t_{rec}$ (ms)	IAE	$\Delta V$ (V)	$t_{rec}$ (ms)	IAE
-50%	21.47	2.80	0.15	15.50	30.10	0.46
+50%	13.97	2.60	0.12	10.89	40.60	0.43
+100%	21.01	3.60	0.14	19.61	47.20	0.54
+150%	26.53	4.50	0.16	26.91	51.60	0.65
+200%	31.03	5.10	0.17	33.25	54.20	0.75

Table 4. Performance Specification Regarding to Input Voltage Variations

Input voltage added in %	Adaptive PI Sliding Surface			PI Sliding Surface		
	$\Delta V$ (V)	$t_{rec}$ (ms)	IAE	$\Delta V$ (V)	$t_{rec}$ (ms)	IAE
-50%	55.70	3.20	0.19	16.69	42.90	0.48
-25%	16.19	2.00	0.12	6.98	34.40	0.38
+25%	7.82	1.80	0.12	5.82	33.00	0.37
+50%	12.76	2.00	0.12	10.92	40.00	0.43
+100%	19.43	2.50	0.13	19.91	46.20	0.54
+125%	22.70	2.80	0.14	23.95	48.00	0.59

## 5. Conclusion

This paper presents a novel technique of controller design using sliding mode control applied for boost control voltage regulation. Based on theoretical proofs and numerical simulation, the proposed method is always able to accurately follow the desired voltage in very short period. In addition, it is more robust in coping the parameter variations compared to another method. Finally, the proposed method consistently produces the least value of IAE and recovery time.

## Acknowledgements

The authors would like to thank to Lembaga Penelitian dan Pengabdian Masyarakat Universitas Brawijaya (LPPM-UB) for providing research grant namely Program Hibah Peneliti Pemula 2018 (Award No. DIPA-042.01.2.400919/2018).

## References

- [1] Subroto RK, Lian KL. Modeling of a Multilevel Voltage Source Converter using the Fast Time-Domain Method. *IEEE Journal of Emerging and Selected Topics in Power Electronics*. 2014; 2(4): 1117-1126.
- [2] Ibrahim O, Yahaya NZ, Saad N. State-space Modeling and Digital Controller Design for DC-DC Converter. *TELKOMNIKA Telecommunication Computing Electronics and Control*. 2016; 14(2): 497-506.
- [3] Samosir AS, Sutikno T, Yatim AHM. Dynamic Evolution Control for Fuel Cell DC-DC Converter. *TELKOMNIKA Telecommunication Computing Electronics and Control*. 2011; 9(1): 183-190.
- [4] Khoygani MRR, Ghasemi R, Sanaei D. Designing Controller for Joined Dynamic Nonlinear PEMFC and Buck Converter System. *International Journal of Power Electronics and Drive System (IJPEDS)*. 2014; 4(2): 137-145.
- [5] Subroto RK, Ardhenta L, Maulana E. A Novel of Adaptive Sliding Mode Controller with Observer for DC/DC Boost Converters in Photovoltaic System. 2017 5<sup>th</sup> International Conference on Electrical, Electronics, and Information Engineering. Malang. 2017: 9-14.



- [6] Naik J. Design and Control for the Buck-Boost Converter Combining 1-Plus-D Converter and Synchronous Rectified Buck Converters. *International Journal of Power Electronics and Drive System (IJPEDS)*. 2015; 6(2): 305-317.
- [7] Sathiyamoorthy S, Gopinath M. A Novel High Gain SEPIC Converter with the Tapped Inductor Model Operating in Discontinuous Conduction Mode for Power Factor Correction. *International Journal of Power Electronics and Drive System (IJPEDS)*. 2016; 7(2): 450-459.
- [8] Amirabadi M. *Cuk-based universal converters in discontinuous conduction mode of operation*. 2016 IEEE Energy Conversion Congress and Exposition (ECCE). Milwaukee. 2016: 1-7.
- [9] Pande SK, Patil SL, Phadke SB, Deshpande AS. *Investigation of sliding mode control of higher order DC-DC converters*. 2016 7th India International Conference on Power Electronics (IICPE). Patiala. 2016: 1-5.
- [10] Mitra L, Swain N. *Closed loop control of solar powered boost converter with PID controller*. 2014 IEEE International Conference on Power Electronics, Drives and Energy Systems (PEDES). Mumbai. 2014: 1-5.
- [11] Sharma K, Palwalia DK. *Design of digital PID controller for voltage mode control of DC-DC converters*. 2017 International Conference on Microelectronics Devices, Circuits and Systems (ICMDCS). Vellore. 2017: 1-6.
- [12] Moreno JS, Mejia EF. *Performance comparison between  $H^\infty$  and PID control strategies applied to Boost power converters*. 2010 IEEE ANDESCON. Bogota. 2010: 1-6.
- [13] Arulsevi S, Uma G, Chidambaram. *Design of PID controller for boost converter with RHS zero*. The 4th International Power Electronics and Motion Control Conference (IPEMC). Xian. 2004: 532-537.
- [14] Li P, Liu R, Ma X. *Adaptive indirect model predictive control schemes for boost converter*. 2017 36th Chinese Control Conference. Dalian. 2017: 9203-9207.
- [15] Cunha MKC, Nogueira FG, Torrico BC. *Self-tuning adaptive controller applied to boost converter voltage control*. 2015 IEEE 13<sup>th</sup> Brazilian Power Electronics Conference and 1<sup>st</sup> Southern Power Electronics Conference (COBEP/SPEC). Fortaleza. 2015: 1-6.
- [16] Qi L, Xiao M. *Robust Control of Boost Converter*. 2017 2nd International Conference on Cybernetics, Robotics and Control (CRC). Chengdu. 2017: 61-65.
- [17] Ouneis F, Golea N.  *$\mu$ -Synthesis based robust voltage control for cascade boost power converter*. 2015 3rd International Conference on Control, Engineering & Information Technology (CIET). Tlemcen. 2017: 1-6.
- [18] Raj RN, Purushotaman KV, Singh NA. *Adaptive TSK-type neural fuzzy controller for boost DC-DC converter*. 2017 IEEE International Conference on Circuits and Systems (ICCS). Thiruvananthapuram. 2017: 441-446.
- [19] Ganeswari JA, Kiranmayi R. *Performance improvement for DC boost converter with fuzzy controller*. 2<sup>nd</sup> International Conference on Inventive Systems and Control (ICISC). Coitambore. 2018: 358-362.
- [20] Krishna SA, Abraham L. *Boost converter based power factor correction for single phase rectifier using fuzzy logic control*. 2014 First International Conference on Computational Systems and Communications (ICCSC). Trivandrum. 2014: 122-126.
- [21] Firdaus AZA, Normahira M, Syahirah KN, Sakinah J. *Design and simulation of Fuzzy Logic Controller for boost converter in renewable energy application*. 2013 IEEE International Conference on Control System, Computing and Engineering. Mindeb. 2013: 520-524.
- [22] Dash SS, Kumar S, Nayak B. *Fuzzy logic controlled PWM boost integrated converter*. 2015 Communication, Control and Intelligent System (CCIS). Mathura. 2015: 318-323.
- [23] Jiao YP, Luo FL. *An Improved Sliding Mode Controller for Boost Converter in Solar Energy System*. 4<sup>th</sup> IEEE Conference on Industrial Electronics and Applications (ICIEA) 2009. Xian. 2009: 805-810.
- [24] Singh S, Fulwani D, Kumar V. Robust sliding – mode control of dc/dc boost converter feeding a constant power load. *IET Power Electronics*. 2015; 8(7): 1230-1237.
- [25] Zhang J, Dorrell DG, Li L, Argha A. *A novel sliding mode controller for dc-dc boost converters under input/load variations*. IECON 2015 – 41<sup>st</sup> Annual Conference of the IEEE Industrial Electronics Society. Yokohama. 2015: 1698-1703.
- [26] He Y, Luo FL. Sliding-mode control for dc-dc converters with constant switching frequency. *IEE Proceedings – Control Theory and Applications*. 2006; 153(1): 37-45.
- [27] Oucheriah S, Guo L. PWM-based adaptive sliding mode control for boost DC/DC converters. *IEEE Transactions on Industrial Electronics*. 2013; 60(8): 3291-3294.
- [28] Jian S, Zhitao L, Hongye S. *A second order sliding mode control design for bidirectional DCDC converter*. 2017 36<sup>th</sup> Chinese Control Conference. Dalian. 2017: 9181-9186.
- [29] Asma C, Abdelaziz Z, Nadia Z. *Dual loop control of DC-DC boost converter based cascade sliding mode control*. 2017 International Conference on Green Energy Conversion Systems (GECS). Hammamet. 2017: 1-6.
- [30] Subroto RK. *Vehicle stability control of 4WD electric vehicle using combined adaptive sliding mode controller and control allocation method*. 2017 IEEE 3<sup>rd</sup> International Future Energy Electronics Conference and ECCE Asia (IFEEEC 2017 – ECCE Asia). Kaohsiung. 2017: 812-817.